THE JOURNAL OF PHYSICAL CHEMISTRY Letters

Letter

pubs.acs.org/JPCL

Seamless and Accurate Modeling of Organic Molecular Materials

Anthony M. Reilly and Alexandre Tkatchenko*

Fritz-Haber-Institut der Max-Planck-Gesellschaft, Faradayweg 4-6, 14195 Berlin, Germany

Supporting Information

ABSTRACT: The near endless possibilities for assembling molecular materials has long posed a difficult challenge for theory. All crystal-structure prediction methods acknowledge the crucial contribution of van der Waals or dispersion interactions, but few go beyond a pairwise additive description of dispersion, ignoring its many-body nature. Here we use two databases to show how a many-body approach to dispersion can seamlessly model both solid and gas-phase interactions within the coveted "chemical accuracy" benchmark, while the underlying pairwise approach fails for solid-state interactions due to the absence of many-body polarization and energy contributions. Our results show that recently developed methods that treat the truly collective nature of dispersion interactions are able to reach the accuracy required for predicting molecular materials, when coupled with nonempirical density functionals.

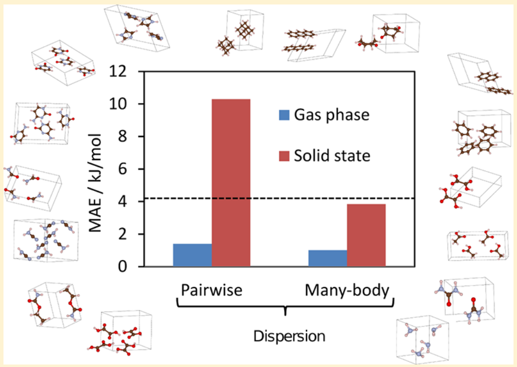

SECTION: Molecular Structure, Quantum Chemistry, and General Theory

Intermolecular interactions are at the heart of all molecular assemblies, controlling the formation of chemical systems such as gas-phase dimers, supramolecular systems, and molecular crystals and materials. In molecular crystals, the intricate nature of hydrogen bonding and van der Waals interactions can give rise to a wide variety of polymorphs and cocrystals for a given molecule.[1] The crystal structure can have a significant impact on the dissolution and bioavailability of an active pharmaceutical ingredient,[2] the formulation of tablets,[3] and the mechanical properties of molecular materials.[4]

Controlling and exploring this vast chemical space is not possible with experimental means alone, and the gauntlet has long been laid down to theory to predict and control the properties of molecular materials.[5] With this challenge, the field of crystal-structure prediction has grown and advanced rapidly[6] with a number of schemes for generating structures remarkably similar to experimentally known ones.[7] However, a number of challenges remain, primarily due to the need for achieving accuracies in relative energies of the order of a few kJ/mol or less.[8] Such energy scales are difficult for all methods, and it is often the case that different methods can give conflicting predictions of relative stabilities.[9] High-level quantum chemical methods are too computationally demanding for crystal-structure prediction, thus empirical potentials and density functional theory (DFT) are the main viable options. Empirical potentials use simple models for the various interactions in molecules, including electrostatics, induction, bond stretching and bending, and dispersion. This gives rise to a large number of parameters that require fitting using experimental or theoretical data. The transferability of the potentials and their suitability for flexible molecules remain serious concerns.[10] DFT is an electronic-structure method, where the electron density and total energy are obtained as the solution of a Hamiltonian describing the fundamental interactions between electrons, with the exchange-correlation functional being central to the success or failure of DFT. As it is dependent on the electron density, DFT can seamlessly model the majority of covalent and noncovalent interactions. As many functionals are semilocal in nature, long-range correlation, including dispersion interactions, are often absent. However, a variety of methods exist for including such interactions within DFT.[11] With a nonempirical exchange-correlation functional, DFT calculations offer a transferable and often accurate picture of molecular interactions.

The importance of including van der Waals or dispersion interactions in both empirical potentials and DFT is now well established.[10,11] These contributions originate from the attractive interaction between instantaneous and induced dipoles (and multipoles) that form due to long-range fluctuations and correlations in electron densities. While these interactions are inherently quantum mechanical in nature, typically they are modeled using pairwise summations of the form[12]

$$E_{\mathrm{disp}} = -\frac{1}{2}\sum_{ij}^{N} f_{\mathrm{damp}}(R_{ij})\frac{C_6}{R_{ij}^{6}} \qquad (1)$$

where C_6 is the leading-order dipole−dipole dispersion coefficient, and R_{ij} is the separation between pairs of atoms i and j. The damping function, $f_{\mathrm{damp}}(R_{ij})$ is used to match the long-range dispersion contributions to the short-range correlation captured by semilocal DFT functionals. Early

Received: January 31, 2013
Accepted: March 12, 2013
Published: March 12, 2013

© 2013 American Chemical Society

dx.doi.org/10.1021/jz400226x | *J. Phys. Chem. Lett.* 2013, 4, 1028−1033

attempts at obtaining C_6 values focused on fitting atomic values to known molecular C_6 values[13] and the use of DFT-calculated ionization potentials and static polarizabilities (DFT-D2[14]). More recently, there are a number of improved methods, such as DFT-D3[15] and DFT+vdW,[16] which rescale accurate free-atom C_6 values based on intrinsic molecular properties such as geometry or Hirshfeld volumes. As such, the pairwise approach to vdW-inclusive DFT is a mature one with a physically motivated description of pairwise dispersion readily available for coupling to DFT, and in recent years DFT-D has seen extensive use for crystal-structure prediction.[7]

Despite the great power and simplicity of the pairwise summation in eq 1 and its widespread use, it is well-known that dispersion interactions represent collective many-body interactions between the instantaneous dipoles and multipoles of atoms,[17] leading to electric-field polarization effects and energy terms stemming from triple-dipole[18] and higher-order interactions.[19] These many-body effects are highly dependent on the environment of atoms and molecules and, as they depend on a self-consistent solution for a system of fluctuating dipoles interacting through the $\sim 1/R^3$ potential, they act over much longer distances than the simplified pairwise expression in eq 1 . A truly predictive approach to molecular-material design requires computational methods that can treat molecules, dimers and solids all on an equal footing. In the present work we show that a recently developed many-body approach to dispersion interactions[20] can seamlessly model both gas-phase and solid-state intermolecular interactions within "chemical accuracy" of 1 kcal/mol, while the underlying pairwise approach is only capable of representing the gas-phase interactions. Coupled with the recent work of Risthaus and Grimme,[21] where three-body terms were found to be essential for modeling supramolecular systems, it becomes increasingly clear that many-body contributions are important in the stability of molecular systems, particularly molecular crystals. The recent work by Otero-de-la-Roza and Johnson,[22] where three-body terms increased errors for molecular crystals, highlights the nontrivial nature of capturing such contributions correctly.

To calculate intermolecular-interaction energies in the pairwise approximation, we employ the DFT+vdW method of Tkatchenko and Scheffler (TS), which rescales free-atom C_6 and polarizabilities values based on the self-consistent electron density.[16] The method yields remarkably accurate C_6 values (5.5% accuracy) for small atomic and molecular dimers.[16] The many-body dispersion (MBD) method[20,23] builds on the TS approach by mapping the TS atomic polarizabilities onto a set of quantum harmonic oscillators (QHOs). In a two-stage process, the electrodynamic response of the system is first obtained using the self-consistent screening (SCS) equations,[24] and the resulting screened QHOs are then coupled using a many-body Hamiltonian that yields all orders of dipole interactions.[20,25] Coupling of the MBD energy to DFT is achieved using a range-separated Coulomb operator to define the MBD dipole-coupling tensors, with only a single empirical parameter required for a given DFT functional.[20]

We couple the TS and MBD methods to the Perdew–Burke–Ernzerhof (PBE)[26] and the hybrid PBE0[27] functionals. PBE is a widely used, well-tested semilocal functional. A well-known deficiency in many such semilocal functionals is the problem of delocalization errors.[28] PBE0 improves on PBE by mixing in a fraction of exact exchange, giving improved modeling of polarizable hydrogen-bonding systems such as ice.[29] We employ nonempirical functionals such as PBE and PBE0 to have a clean match between the TS and MBD dispersion energies and the short-range DFT correlation. Empirical functionals may partly parametrize the long-range correlation leading to spurious behavior when coupled to the physically grounded dispersion terms. Many DFT functionals have appreciable *absolute* errors in their short-range many-body correlation[30] and may also be inadequate for modeling the short-ranged multipole vdW contributions (C_8/R^8, etc.). For this reason, a number of pairwise methods employ C_8/R^8 and C_{10}/R^{10} terms in eq 1.[15,31] There is evidence that such interactions are captured by nonempirical DFT functionals (like PBE and PBE0) to a good degree,[32−34] except for materials under relatively high pressure.[29] The recent work of Mardirossian et al.[35] has shown worse performance for XDM with C_8 and C_{10} terms for sulfate−water cluster binding energies than with only C_6 contributions. As we shall see, the main issue for pairwise methods in molecular crystals is overestimation of the dispersion energy,[31] and the attractive multipole terms would only exacerbate this.

There are a number of benchmark data sets for gas-phase intermolecular interactions, obtained from coupled-cluster theory with singles, doubles, and perturbative triples [CCSD(T)], the widely accepted "gold standard" for quantum-chemical calculations.[36] In particular, the damping function and range-separation parameters of the TS and MBD methods, respectively, are fitted to the S22 data set of 22 gas-phase dimers.[37] The performance of both methods can then be best assessed using the larger S66×8 database,[38] which has 66 gas-phase dimers at eight different intermolecular separations (528 geometries in total). The latter makes this database a stern test, as the S22 considers only equilibrium separations. The resulting deviations from the S66×8 binding energies are detailed in Table 1, while the values for the different classes of interactions are given in Table S1. The highly coveted "chemical accuracy" target is to have deviations of less than 4.2 kJ/mol (1 kcal/mol). PBE+TS easily achieves this goal, with a mean absolute error (MAE) of 1.54 kJ/mol. The maturity of pairwise correction methods can be further seen in the comparable performance for other schemes (e.g., MAE for PBE+D3(BJ) with S66 × 8 is 1.46 kJ/mol[39]). Nevertheless, there is a marked improvement when using MBD compared to TS. In particular, as has been seen for the S22,[20] MBD substantially improves the performance for the dispersion and mixed/other systems, reducing the dispersion bound MAE from 1.94 kJ/mol (PBE+TS) to 1.26 kJ/mol (PBE+MBD). The improvement for the hydrogen-bonded systems is slightly smaller, and, overall, the relative errors of the three classes become closer to one another. The role of MBD in these systems is to included three-

Table 1. The MAE, Standard Deviation (SD), and MARE of Different vdW-Inclusive DFT Methods with Respect to the CCSD(T) Binding Energies of the S66×8 Database[a]

	MAE (kJ/mol)	SD (kJ/mol)	MARE (%)
PBE+TS	1.54	1.66	13.6
PBE0+TS	1.40	1.61	11.2
PBE+MBD	1.09	1.54	9.8
PBE0+MBD	1.01	1.56	8.5

[a] In the analysis, the eight binding distances are given equal weight. Calculations were performed using the FHI-aims code[40] in the fashion described elsewhere.[20,23]

body and higher terms that are important for binding but cannot be mimicked by a pairwise term alone.[23] MBD also captures some of the anisotropy of the dispersion interactions, which are completely neglected by C_6/R^6-type models. PBE0 improves on the PBE energies, not just for hydrogen-bonded systems but also for dispersion and mixed systems most likely due to its smaller short-range many-body correlation error.[30]

Turning to the solid state, there are no established high-level theoretical benchmark data sets for molecular crystals due to the greater computational cost and complexity of solid-state calculations. Therefore, the lattice energy (defined as the energy difference between a molecule being in the crystal and the gas phase) is often compared with experimental enthalpies of sublimation.[31] Careful comparison between the two quantities requires evaluation of a number of contributions:

$$\Delta H_{\rm sub}(T) = -E_{\rm latt} + (E_{\rm ZPE,gas} - E_{\rm ZPE,solid}) + \int_0^T \Delta C_{\rm p}(T)\,{\rm d}T + \sum \Delta H_{\rm trans} \qquad (2)$$

where $E_{\rm ZPE}$ is the zero-point vibrational energy, $\Delta C_{\rm p}$ is the difference between the gas-phase and solid-state heat capacities, and $H_{\rm trans}$ is the enthalpy of transformation for any phase transition that occurs between 0 K and T. In the ideal-gas, rigid-rotor, and harmonic approximations, this reduces to

$$\Delta H_{\rm sub}(T) = -E_{\rm latt} + E_{\rm vib,gas}(T) - E_{\rm vib,solid}(T) + 4RT \qquad (3)$$

where $E_{\rm vib}$ is the total (thermal and zero-point) vibrational energy. To form a small but representative database, we have taken 16 molecular crystals (hereafter referred to as the X16) from the database of Otero-de-la-Roza and Johnson[31] and calculated lattice energies using both the pairwise and MBD approaches coupled to the PBE and PBE0 functionals. Calculations were performed using the CASTEP plane-wave DFT code.[41,42] The database is illustrated in Figure 1 and contains a number of examples of vdW-bound systems such as benzene and adamantane, a number of hydrogen-bonded systems, including urea and ammonia, as well some mixed systems, such as imidazole and uracil.

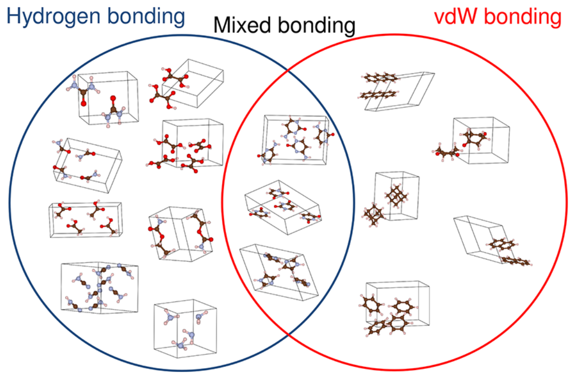

Figure 1. Types and structures of the 16 molecular crystals in the X16 database.

As such, the database represents the key interactions in molecular crystals and features both small high-symmetry systems (suitable for more sophisticated computational methods) as well as some larger molecules that better represent the target systems of crystal-structure prediction. To enable a direct comparison with enthalpies of sublimation at 298 K, the vibrational terms in eq 3 have been determined using DFT phonon calculations (see Supporting Information for more details). For naphthalene,[43] adamantane,[44] anthracene,[45] and urea,[46] experimental $C_{\rm p}$ data are available for the solid state and have been used in conjunction with DFT-calculated $C_{\rm p}$ values for the isolated molecules to evaluate the integral in eq 2, which together with DFT-calculated zero-point energies gives a semianharmonic value for the experimental lattice energy.

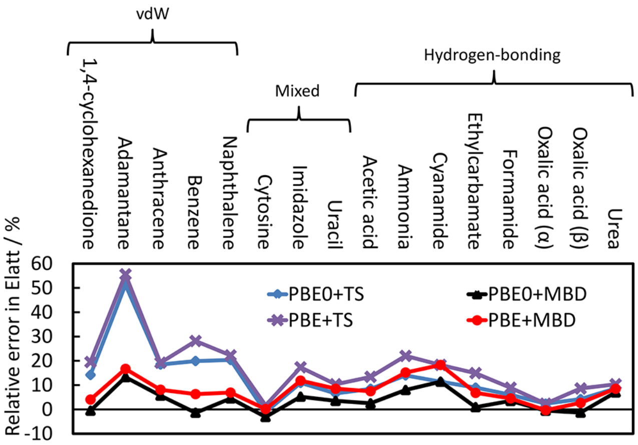

Figure 2. The relative error in the prediction of the lattice energy of 16 molecular crystals using DFT calculations augmented with pairwise and many-body van der Waals energies.

Table 2. The MAE, SD, and MARE of Different vdW-Inclusive DFT Methods with Respect to Experimental Lattice Energies of the X16 Molecular Crystals

	MAE (kJ/mol)	SD (kJ/mol)	MARE (%)
PBE+TS	13.57	8.38	17.16
PBE0+TS	10.25	8.40	12.91
PBE+MBD	6.37	3.98	7.92
PBE0+MBD	3.84	4.01	4.52

The performance of the different approaches for each crystal is illustrated in Figure 2, while a statistical summary is presented in Table 2. Unlike for the gas-phase dimers, there is a much larger difference in the performance for the pairwise and many-body schemes. As has been noted elsewhere,[31] pairwise PBE+TS significantly overestimates lattice energies, and for the X16 has a mean absolute error over three times the "chemical accuracy" target. However, here we show that using PBE+MBD leads to a dramatic improvement in the prediction of lattice energies, more than halving the MAE. Coupling MBD to the PBE0 functional instead of PBE further improves the MBD results. The contribution of MBD is not simply to broadly reduce the pairwise dispersion energy, it is clearly specific to certain systems and geometries, with some systems such as adamantane having very large corrections (27 kJ/mol) and others being virtually unchanged. The X16 database contains two polymorphs of oxalic acid (α and β), which experimentally have sublimation enthalpies and lattice energies within 1 kJ/mol of one another.[31] PBE+TS overestimates the β-form stability by 4 kJ/mol relative to the α form. Other pairwise methods (D2 and XDM[31]) have also been shown to overestimate the β form stability by a comparable amount.

Despite their similar structures, which yield virtually identical lattice energies, the MBD reduction in the lattice energy of the β form is twice that of the α form, correctly restoring the near degeneracy of the two forms and bring them within a few percent of the experimental values. This illustrates the sensitivity of the MBD energy to the internal structure of the crystal. The PBE0+MBD approach has also been shown to correctly model the polymorphism in glycine, another system that poses great difficulties for pairwise methods.[47]

Overall, PBE0+MBD reaches a remarkable accuracy of 3.8 kJ/mol, within the elusive "chemical accuracy" target of 4.2 kJ/mol and also featuring a mean absolute relative error (MARE) of only 4.5%. For hydrogen-bonded systems, the natural delocalization within the bulk limits the impact of DFT delocalization errors,[33] reducing the potential for cancellation of errors. The systematic decrease in lattice energies with PBE0 can then be partly understood as a relative stabilizing of the isolated molecules. The lower overestimation of short-range many-body correlation in PBE0 will also play a role.[30] It is important to stress that MBD has only a single fitted parameter, the range-separation parameter, which is determined solely by fitting to the S22 gas-phase dimer database for a given functional. The good performance of MBD for both solids and dimers is a strong validation of both the method and the importance of including collective dispersion interactions in computational models of molecular systems.

We note that using the experimental C_p data for adamantane, anthracene, naphthalene, and urea, leads to increases in lattice energies of 2−3 kJ/mol for these systems, leading to better agreement with the PBE0+MBD values. Such a trend repeated for the other systems would give even better agreement, but we are content to be within the estimated experimental uncertainty of sublimation-enthalpy measurements (4.9 kJ/mol[48]). To illustrate the importance of MBD for larger, pharmaceutically relevant molecules we have also calculated the lattice energy of form-I aspirin. The PBE+TS value is −147.1 kJ/mol, while the PBE0+MBD value is −135.5 kJ/mol, a reduction of nearly three times the "chemical accuracy" target. The PBE0+MBD value agrees with the SCS(MI) RI-MP2 value of Wen and Beran[49] (within 0.1 kJ/mol). The challenge of polymorphism will often require even greater accuracy than shown here (of the order of 1 kJ/mol).[8] The uncertainties in experimental data do not permit a critical assessment of such an accuracy, but in reaching "chemical accuracy" in the absolute lattice energies, there is hope that MBD relative energies will have a substantially lower error.

Looking at the individual systems more closely, one can start to understand where many-body effects will be important. It is clear from Figure 2 that MBD is essential for modeling vdW-bound systems, with very large corrections to lattice energies that yield substantial improvements in the DFT predictions. The reduction in lattice energy arises from many-body screening of the vdW energy. Figure 3 shows the ellipsoidal representation of the anisotropic screened polarizability tensors of a molecule from the form-I aspirin crystal structure, obtained from the SCS equations. The ellipsoids show how short-range screening leads to significant polarization along the chemical bonds of the molecule, deviating greatly from the isotropic picture inherent to most pairwise approaches. However, this intramolecular polarization effect largely cancels as the internal molecular structure usually varies little between the crystal and isolated molecule. In contrast, the long-range screening of the dipole interactions leads to a reduction in the dispersion energy in the solid state. Using the screened polarizabilities in the Casimir-Polder integral[50] we find that the average C-atom C_6 coefficient of aspirin is approximately 10% smaller in the crystal than in the isolated molecule. The greater importance of MBD for solids can be illustrated further by considering systems present in both the S66×8 and the X16. For example, the difference between the PBE+TS and PBE+MBD binding energies of acetic acid amounts to less than 1% at equilibrium in the S66×8 (rising to 3.5% at the longest separation), which is expected given the hydrogen-bonding nature of the dimer. However, in the molecular crystal, the MBD contribution is already over 5% at equilibrium. While the TS method has excellent molecular C_6 coefficients for small gas-phase molecules and performs well for the S22 and S66 gas-phase dimers,[16,20,23] it neglects the long-range screening effects crucial to solid-state interactions and therefore greatly overestimates the solid-state dispersion energy for vdW-bound systems. Indeed, screening of polarizabilities is not only important for energies but also has a significant impact on the dielectric properties of such molecular crystals, and the SCS approach has been recently shown to correctly predict the dielectric constants of the polyacene crystals.[51]

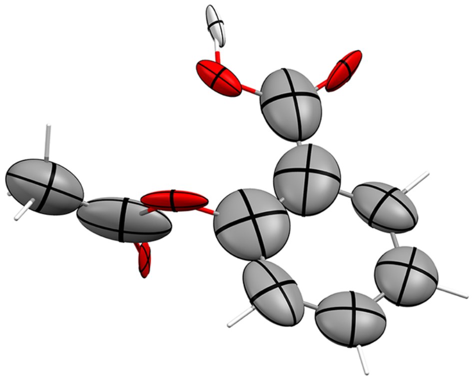

Figure 3. Ellipsoidal representation of the atomic polarizability tensors obtained from the solution of the self-consistent screening equation for a molecule from the crystal structure of form-I aspirin. For clarity, the tensors for H atoms bonded to C atoms, which polarize strongly along the C−H bonds, are omitted.

In the present study we have demonstrated that the PBE0+MBD method performs excellently for predicting gas-phase dimer binding energies and molecular-crystal lattice energies, while the underlying pairwise TS approach systematically overestimates the latter. The use of DFT, in particular a nonempirical hybrid functional, ensures a first-principles description of short-range interactions and repulsion between atoms, while the TS method is an excellent source of hybridized polarizabilities. While some of the MBD contribution to crystal stability could be captured by fitting or adjusting pairwise vdW coefficients or the damping function,[31] the MBD scheme provides a physically motivated method for modeling such contributions in a seamless and transferable fashion, broadly improving the performance of simple pairwise methods. The cost of MBD energy evaluation is negligible compared to the underlying DFT calculation, involving simple operations on $3N \times 3N$ matrices, where N is the numbers of atoms in the system. Currently, efforts are in progress to obtain analytic expressions for derivatives and stresses for the DFT+MBD method. Crystal-structure prediction is often a hierarchical approach, with empirical potentials being used to generate many trial structures, the most promising of which are then ranked by

DFT.[7] Coupling MBD to polarizable or multipole force fields could also lead to significant improvements in the ranking of polymorphs in the early steps of crystal-structure prediction, allowing for more accurate and computationally demanding DFT treatments (such as nonempirical hybrid functionals) to become routinely and widely used in the latter stages of crystal-structure prediction.

■ ASSOCIATED CONTENT

Ⓢ Supporting Information

A table of calculated lattice energies, experimental sublimation enthalpies and vibrational contributions, along with a detailed computational methodology and archive file containing PBE+TS optimized geometries and Hirshfeld volumes for the X16 systems and aspirin and the binding energies for the S66×8 database with the four methods discussed here. This material is available free of charge via the Internet at http://pubs.acs.org/.

■ AUTHOR INFORMATION

Corresponding Author

*E-mail: tkatchen@fhi-berlin.mpg.de.

Notes

The authors declare no competing financial interest.

■ ACKNOWLEDGMENTS

The authors acknowledge support from the European Research Council (ERC Starting Grant VDW-CMAT).

■ REFERENCES

(1) Bernstein, J. *Polymorphism in Molecular Crystals; International Union of Crystallography*; Oxford University Press: New York, 2007.

(2) Blagden, N.; de Matas, M.; Gavan, P.; York, P. Crystal Engineering of Active Pharmaceutical Ingredients to Improve Solubility and Dissolution Rates. *Adv. Drug Delivery Rev.* **2007**, *59*, 617−630.

(3) Karki, S.; Friščić, T.; Fábián, L.; Laity, P. R.; Day, G. M.; Jones, W. Improving Mechanical Properties of Crystalline Solids by Cocrystal Formation: New Compressible Forms of Paracetamol. *Adv. Mater.* **2009**, *21*, 3905−3909.

(4) Reddy, C. M.; Rama Krishna, G.; Ghosh, S. Mechanical Properties of Molecular Crystals—Applications to Crystal Engineering. *CrystEngComm* **2010**, *12*, 2296−2314.

(5) Maddox, J. Crystals from first principles. *Nature* **1988**, *335*, 201.

(6) Neumann, M. A.; Leusen, F. J. J.; Kendrick, J. A Major Advance in Crystal Structure Prediction. *Angew. Chem., Int. Ed.* **2008**, *47*, 2427−2430.

(7) Bardwell, D. A.; Adjiman, C. S.; Arnautova, Y. A.; Bartashevich, E.; Boerrigter, S. X. M.; Braun, D. E.; Cruz-Cabeza, A. J.; Day, G. M.; Della Valle, R. G.; Desiraju, G. R.; et al. Towards Crystal Structure Prediction of Complex Organic Compounds – A Report on the Fifth Blind Test. *Acta Crystallogr. B* **2011**, *67*, 535−551.

(8) Price, S. L. Computed Crystal Energy Landscapes for Understanding and Predicting Organic Crystal Structures and Polymorphism. *Acc. Chem. Res.* **2009**, *42*, 117−126.

(9) Wen, S.; Beran, G. J. O. Crystal Polymorphism in Oxalyl Dihydrazide: Is Empirical DFT-D Accurate Enough? *J. Chem. Theory Comput.* **2012**, *8*, 2698−2705.

(10) Stone, A. J. Intermolecular Potentials. *Science* **2008**, *321*, 787−789.

(11) Klimeš, J.; Michaelides, A. Perspective: Advances and Challenges in Treating van der Waals Dispersion Forces in Density Functional Theory. *J. Chem. Phys.* **2012**, *137*, 120901.

(12) Grimme, S. Density Functional Theory with London Dispersion Corrections. *Comput. Mol. Sci.* **2011**, *1*, 211−228.

(13) Neumann, M. A.; Perrin, M.-A. Energy Ranking of Molecular Crystals Using Density Functional Theory Calculations and an Empirical van der Waals Correction. *J. Phys. Chem. B* **2005**, *109*, 15531−15541.

(14) Grimme, S. Semiempirical GGA-Type Density Functional Constructed with a Long-Range Dispersion Correction. *J. Comput. Chem.* **2006**, *27*, 1787−1799.

(15) Grimme, S.; Antony, J.; Ehrlich, S.; Krieg, H. A Consistent and Accurate Ab Initio Parametrization of Density Functional Dispersion Correction (DFT-D) for the 94 Elements H−Pu. *J. Chem. Phys.* **2010**, *132*, 154104.

(16) Tkatchenko, A.; Scheffler, M. Accurate Molecular van der Waals Interactions from Ground-State Electron Density and Free-Atom Reference Data. *Phys. Rev. Lett.* **2009**, *102*, 073005.

(17) Dobson, J. F.; Gould, T. Calculation of Dispersion Energies. *J. Phys.: Condens. Matter* **2012**, *24*, 073201.

(18) Axilrod, B. M.; Teller, E. Interaction of the van der Waals Type between Three Atoms. *J. Chem. Phys.* **1943**, *11*, 299−300.

(19) Bade, W. L. Drude-Model Calculation of Dispersion Forces. I. General Theory. *J. Chem. Phys.* **1957**, *27*, 1280−1284.

(20) Tkatchenko, A.; DiStasio, R. A.; Car, R.; Scheffler, M. Accurate and Efficient Method for Many-Body van der Waals Interactions. *Phys. Rev. Lett.* **2012**, *108*, 236402.

(21) Risthaus, T.; Grimme, S. Benchmarking of London Dispersion-Accounting Density Functional Theory Methods on Very Large Molecular Complexes. *J. Chem. Theory Comput.* **2013**, DOI: 10.1021/ct301081n.

(22) Otero-de-la-Roza, A.; Johnson, E. R. Many-Body Dispersion Interactions from the Exchange-Hole Dipole Moment Model. *J. Chem. Phys.* **2013**, *138*, 054103.

(23) DiStasio, R. A.; von Lilienfeld, O. A.; Tkatchenko, A. Collective Many-Body van der Waals Interactions in Molecular Systems. *Proc. Natl. Acad. Sci. U.S.A.* **2012**, *109*, 14791−14795.

(24) Mayer, A. Formulation in Terms of Normalized Propagators of a Charge-Dipole Model Enabling the Calculation of the Polarization Properties of Fullerenes and Carbon Nanotubes. *Phys. Rev. B* **2007**, *75*, 045407.

(25) Cole, M. W.; Velegol, D.; Kim, H.-Y.; Lucas, A. A. Nanoscale van der Waals Interactions. *Mol. Simul.* **2009**, *35*, 849−866.

(26) Perdew, J. P.; Burke, K.; Ernzerhof, M. Generalized Gradient Approximation Made Simple. *Phys. Rev. Lett.* **1996**, *77*, 3865−3868.

(27) Adamo, C.; Barone, V. Toward Reliable Density Functional Methods without Adjustable Parameters: The PBE0 Model. *J. Chem. Phys.* **1999**, *110*, 6158−6170.

(28) Cohen, A. J.; Mori-Sánchez, P.; Yang, W. Insights into Current Limitations of Density Functional Theory. *Science* **2008**, *321*, 792−794.

(29) Santra, B.; Klimeš, J.; Alfè, D.; Tkatchenko, A.; Slater, B.; Michaelides, A.; Car, R.; Scheffler, M. Hydrogen Bonds and van der Waals Forces in Ice at Ambient and High Pressures. *Phys. Rev. Lett.* **2011**, *107*, 185701.

(30) Tkatchenko, A.; von Lilienfeld, O. A. Popular Kohn−Sham Density Functionals Strongly Overestimate Many-Body Interactions in van der Waals systems. *Phys. Rev. B* **2008**, *78*, 045116.

(31) Otero-de-la-Roza, A.; Johnson, E. R. A Benchmark for Non-covalent Interactions in Solids. *J. Chem. Phys.* **2012**, *137*, 054103.

(32) Marom, N.; Tkatchenko, A.; Rossi, M.; Gobre, V. V.; Hod, O.; Scheffler, M.; Kronik, L. Dispersion Interactions with Density-Functional Theory: Benchmarking Semiempirical and Interatomic Pairwise Corrected Density Functionals. *J. Chem. Theory Comput.* **2011**, *7*, 3944−3951.

(33) Steinmann, S. N.; Corminboeuf, C. Exploring the Limits of Density Functional Approximations for Interaction Energies of Molecular Precursors to Organic Electronics. *J. Chem. Theory Comput.* **2012**, *8*, 4305−4316.

(34) Steinmann, S. N.; Piemontesi, C.; Delachat, A.; Corminboeuf, C. Why Are the Interaction Energies of Charge-Transfer Complexes Challenging for DFT? *J. Chem. Theory Comput.* **2012**, *8*, 1629−1640.

(35) Mardirossian, N.; Lambrecht, D. S.; McCaslin, L.; Xantheas, S. S.; Head-Gordon, M. The Performance of Density Functionals for Sulfate−Water Clusters. *J. Chem. Theory Comput.* **2013**, *9*, 1368−1380.

(36) Raghavachari, K.; Trucks, G. W.; Pople, J. A.; Head-Gordon, M. A Fifth-Order Perturbation Comparison of Electron Correlation Theories. *Chem. Phys. Lett.* **1989**, *157*, 479−483.

(37) Jurečka, P.; Šponer, J.; Černý, J.; Hobza, P. Benchmark Database of Accurate (MP2 and CCSD(T) Complete Basis Set Limit) Interaction Energies of Small Model Complexes, DNA Base Pairs, and Amino Acid Pairs. *Phys. Chem. Chem. Phys.* **2006**, *8*, 1985−1993.

(38) Řezáč, J.; Riley, K. E.; Hobza, P. S66: A Well-Balanced Database of Benchmark Interaction Energies Relevant to Biomolecular Structures. *J. Chem. Theory Comput.* **2011**, *7*, 2427−2438.

(39) Goerigk, L.; Kruse, H.; Grimme, S. Benchmarking Density Functional Methods against the S66 and S66×8 Datasets for Non-Covalent Interactions. *ChemPhysChem* **2011**, *12*, 3421−3433.

(40) Blum, V.; Gehrke, R.; Hanke, F.; Havu, P.; Havu, V.; Ren, X.; Reuter, K.; Scheffler, M. Ab Initio Molecular Simulations with Numeric Atom-Centered Orbitals. *Comput. Phys. Commun.* **2009**, *180*, 2175−2196.

(41) Clark, S. J.; Segall, M. D.; Pickard, C. J.; Hasnip, P. J.; Probert, M. I. J.; Refson, K.; Payne, M. C. First-Principles Methods Using CASTEP. *Z. Kristallogr.* **2005**, *220*, 567−570.

(42) McNellis, E. R.; Meyer, J.; Reuter, K. Azobenzene at Coinage Metal Surfaces: Role of Dispersive van der Waals Interactions. *Phys. Rev. B* **2009**, *80*, 205414.

(43) McCullough, J. P.; Finke, H. L.; Messerly, J. F.; Todd, S. S.; Kincheloe, T. C.; Waddington, G. The Low-Temperature Thermodynamic Properties of Naphthalene, l-Methylnaphthalene, 2-Methylnaphthalene, 1,2,3,4-Tetrahydronaphthalene, *trans*-Decahydronaphthalene and *cis*-Decahydronaphthalene. *J. Phys. Chem.* **1957**, *61*, 1105−1116.

(44) Chang, S.-S.; Westrum, E. F. Heat Capacities and Thermodynamic Properties of Globular Molecules. I. Adamantane and Hexamethylenetetramine. *J. Phys. Chem.* **1960**, *64*, 1547−1551.

(45) Goursot, P.; Girdhar, H. L.; Westrum, E. F. Thermodynamics of Polynuclear Aromatic Molecules. III. Heat Capacities and Enthalpies of Fusion of Anthracene. *J. Phys. Chem.* **1970**, *74*, 2538−2541.

(46) Andersson, O.; Matsuo, T.; Suga, H.; Ferloni, P. Low-Temperature Heat Capacity of Urea. *Int. J. Thermophys.* **1993**, *14*, 149−158.

(47) Marom, N.; DiStasio, R. A.; Atalla, V.; Levchenko, S.; Chelikowsky, J. R.; Leiserowitz, L.; Tkatchenko, A. Many-Body Dispersion Interactions in Molecular Crystal Polymorphism. *ArXiv e-Print Arch., Condens. Matter* **2012**, DOI: arXiv:1210.5636.

(48) Chickos, J. S. Enthalpies of Sublimation after a Century of Measurement: A View as Seen through the Eyes of a Collector. *Netsu Sokutei* **2003**, *30*, 125−130.

(49) Wen, S.; Beran, G. J. O. Accidental Degeneracy in Crystalline Aspirin: New Insights from High-Level ab Initio Calculations. *Cryst. Growth Des.* **2012**, *12*, 2169−2172.

(50) Casimir, H. B. G.; Polder, D. The Influence of Retardation on the London−van der Waals Forces. *Phys. Rev.* **1948**, *73*, 360−372.

(51) Schatschneider, B.; Liang, J.-J.; Reilly, A. M.; Marom, N.; Zhang, G.-X.; Tkatchenko, A. Electrodynamic Response and Stability of Molecular Crystals. *Phys. Rev. B* **2013**, *87*, 060104.